

# Adsorptive Removal of Uranium from Water by Sulfonated Phenol–Formaldehyde Resin

Gülten Atun, Sinem Ortoboy

Department of Chemistry, Faculty of Engineering, Istanbul University, Avcilar, Istanbul, Turkey

Received 10 September 2008; accepted 15 June 2009

DOI 10.1002/app.31004

Published online 17 August 2009 in Wiley InterScience (www.interscience.wiley.com).

**ABSTRACT:** Adsorption characteristics of a sulfonated phenol-formaldehyde resin (SPR) have been studied for U removal from aqueous solution by means of batch method. Adsorption experiments have been carried out as a function of contact time, solution/adsorbent ratio, particle size and pH. Adsorption isotherm has been evaluated by changing adsorbent dosage in the range of 0.04–80 g/L at an initial uranyl nitrate concentration of 0.05 mol/L. The enormous adsorption capacity of 0.29 mol/g estimated from the plateau region of the S shaped isotherm is well comparable the Langmuir capacity of 0.31 mol/g. Equilibrium data are also adequately well described by the Freundlich and the Dubinin-Radushkevich (D-R) isotherm

equations. The parameters of the isotherms and pH dependency of distribution coefficients ( $K_D$ ) indicate that polymeric uranyl chains form on bidentate surface complex as a result of solute–solute interactions on the adsorbent surface. Both desorption and elution studies show that uranyl chains are irreversibly bounded on the SPR. Kinetic curves having a fast initial part followed by a slower process well fit both McKay model based on two-resistance diffusion and Nernst-Planck model with single diffusion coefficient. © 2009 Wiley Periodicals, Inc. *J Appl Polym Sci* 114: 3793–3801, 2009

**Key words:** adsorption; diffusion; waste; chain; resins

## INTRODUCTION

Uranium adsorption is an important treatment method for purification of contaminated solutions and for ultimate disposal of radioactive wastes but it is a complex phenomenon because uranyl-ion  $\text{UO}_2^{2+}$  may be present in different hydrolyzed forms depending on solution pH and concentration. The uranium species in aqueous solution are  $\text{UO}_2^{2+}$ ,  $\text{UO}_2(\text{OH})^+$ ,  $\text{UO}_2(\text{OH})_2^0$  and  $\text{UO}_2(\text{OH})_3^-$  in the pH range of 1–8 whereas its main species in neutral and slightly alkaline natural waters are  $\text{UO}_2(\text{CO}_3)_2^{2-}$  and  $\text{UO}_2(\text{CO}_3)_3^{4-}$ .<sup>1–3</sup> Uranium also exists mainly as the stable anionic tricarbonat-uranyl complex in natural sea water having slightly alkaline pH.<sup>4–8</sup> Organic exchangers used for U removal from sea water have been classified into three types: a chelating ion-exchange resin containing amidoxime functional groups, a macrocyclic compound bounded to a resin and a cellulose resin immobilized by polyphenol compounds.<sup>4–12</sup>

Styrene-divinylbenzene exchangers containing different functional groups have been examined for U removal to obtain drinking water from three ground water simulants.<sup>3</sup> In general, their affinity sequences based on distribution coefficients ( $K_D$ ) decrease in

following order,  $\text{R}-\text{N}(\text{CH}_3)_3\text{OH} > \text{R}-\text{N}(\text{CH}_3)_2 > \text{R}-\text{CH}_2\text{NHCH}_2\text{PO}_3\text{H}_2 > \text{R}-\text{N}(\text{CH}_2\text{COOH})_2 > \text{R}-\text{COOH} > \text{R}-\text{SO}_3\text{H}$ . Strong base anion exchanger resin,  $\text{R}-\text{N}(\text{CH}_3)_3\text{OH}$ , has the highest  $K_D$  value for U which is present in anionic carbonate form whereas it is hardly adsorbed on strong acid cation exchanger,  $\text{R}-\text{SO}_3\text{H}$ . However, other cation exchangers can remove uranium as uranyl cation by stripping carbonate complex.

A recently prepared sulfonated phenol formaldehyde resin has been successfully used as an adsorbent for cationic dyes.<sup>13</sup> It may also have a potential for U removal in  $\text{UO}_2^{2+}$  form at low pH region.

## EXPERIMENTAL

### Materials and methods

The sulfonated phenol-formaldehyde resin (SPR) used as an adsorbent in this study was supplied from Chemical Engineering Department of Istanbul University. The specifications of the SPR have already been reported.<sup>13</sup> All other chemicals were purchased from Merck (Darmstadt, Germany).

The particle density of the SPR was determined as 1.54 g/mL by using a Wertheim pycnometer of 10 mL capacity coupled with a thermometer. The estimated uncertainty of the measured density is  $\pm 0.01$  g/mL at 298 K.

The SPR was grounded and dry-sieved under laboratory atmosphere to give grain sizes  $d < 40 \mu$ ,  $40 \mu$

Correspondence to: G. Atun (gultena@istanbul.edu.tr).

$d < 150 \mu$  and  $d > 150 \mu$  before used in adsorption studies.

Kinetic studies were performed with three different particle sizes of the SPR for determining equilibrium time at a solution/solute ratio of 0.5 L/g. Thus, 0.02 g of the adsorbents was contacted with 10 mL of the 0.05 M uranyl-nitrate solution in a thermostatic shaker/water bath at 298 K for varying time intervals until 1500 min. Solution was separated from the solid phase by centrifugation at 7000 rpm and analyzed for  $\beta$  activity so as to calculate U concentration. For this purpose, 2 mL of supernatant was evaporated in Al capsules and its activity was measured with an ERD Mullard G-M counter MX 123. Each experiment was performed duplicate and five replicate measurements were made in each case for calculation of the mean activities. Standard deviations were less than 3.5%. Concentration of the solution was determined from the calibration curve constructed between the mean activity and U concentration. Calibration curve passing through origin was strictly linear up to 0.1 M U concentration (not shown here, the slope: 22,477 cpm L/mol,  $r^2 = 0.9998$ ).

Although amount of adsorbed U increased by decreasing particle size further experiments were performed with the particle size of  $40 \mu < d < 150 \mu$  because it was more easily separated with centrifugation than the lower size fraction. Kinetic studies were also conducted at the solution/solid ratio of 7.5 L/g using 75 mL U solution and 0.01 g of the SPR. The loaded adsorbents were contacted with the equal volume of 0.1 M  $\text{NaNO}_3$  solutions for time dependent elution studies.

To obtain relevant data for isotherms, adsorption equilibria were investigated by changing solution/adsorbent ratio in the range of 0.0125–25 L/g at 0.05 M uranyl-nitrate concentration. The loaded adsorbents were also recontacted with distilled water at the same water/adsorbent ratios for desorption tests.

Effect of pH on U adsorption was studied at  $V/m$  ratio of 7.5 L/g. Natural pH of 0.05 M uranyl-nitrate solution is  $\sim 2$ . The initial pHs of solutions were adjusted with 1 N  $\text{HNO}_3$  and 0.1 N  $\text{NaOH}$  in the range of 0.739–3.250. A precipitate was observed at higher pH values in uranyl nitrate solution. Ionic strength of 0.05 M  $\text{UO}_2(\text{NO}_3)_2$  solutions was also kept constant at 0.25 M by adding required amount of  $\text{NaNO}_3$ . Equilibrium pHs of the solutions ( $\text{pH}_e$ ) were also recorded. The pH measurements were made using a Jenway pH meter equipped with a combined glass electrode.

Experiments were also performed in uranyl acetate solution to compare anion effect on U adsorption at the  $V/m$  ratios of 0.5 and 1.0 L/g, respectively.

## RESULTS AND DISCUSSION

### Kinetics of uranium adsorption

Time dependent uranium adsorption for three different particle sizes of the SPR at a solution/solid ratio of 0.5 L/g has been calculated from the following relation and presented in Figure 1(a).

$$q_t = C_0 F_t \frac{V}{m} \quad (1)$$

where,  $q_t$  is amount of U adsorbed per unit weight of adsorbent (in mol/g),  $C_0$  is initial solution concentration (in mol/L),  $V/m$  is solution/adsorbent ratio

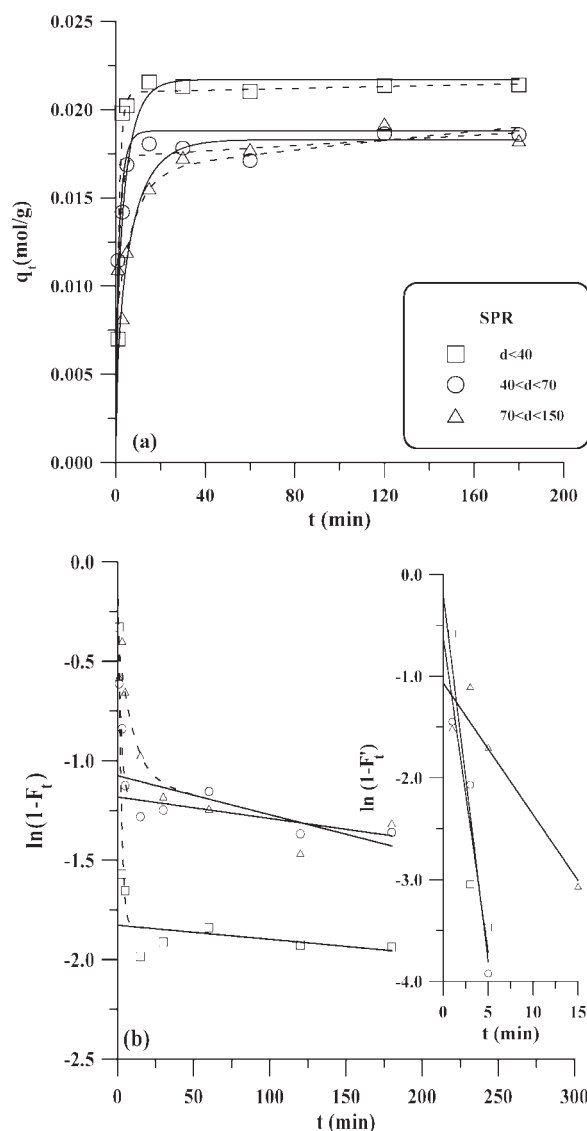


**Figure 1** (a) Time dependencies of U adsorbed on the SPR with different particle sizes at the  $V/m$  ratio of 0.5 L/g. (b) McKay plots for calculation  $k_2$  and  $D_p$ , the inset: McKay plots for calculation  $k_1$  and  $D_f$  (the dashed and the solid curves in (a) have been calculated using the McKay and Nernst-Planck constants, respectively).

(L/g) and  $F_t$  is time dependent adsorbed fraction calculated as follows:

$$F_t = \frac{C_0 - C_t}{C_0} \quad (2)$$

$$F_t = \frac{\bar{C}_t}{C_0} \quad (3)$$

where,  $C_t$  is adsorbate concentration at time  $t$ , so  $\bar{C}_t$  is the concentration in solid phase (in mol/L).

As shown in Figure 1(a), a slower process follows a rapid initial uptake. McKay and Nernst-Plank equations could be applied to the kinetic data based on two- and one-resistance diffusion models, respectively.<sup>14-17</sup>

### McKay Model

McKay equation, which assumes film- and particle diffusion, can be written as follows,<sup>14,15</sup>

$$\ln(1 - F_t) = -k_1(C_t + \bar{C}_t)t \quad (4)$$

To analyze the  $\ln(1 - F_t) = f(t)$  curves in Figure 1(b) plotted according to McKay equation the final linear portion is extrapolated back to  $t = 0$ . A straight line represented in the inset in Figure 1(b), whose slope is correlated to the rate constant of initial fast process ( $k_1$ , in L/mol s), is obtained subtracting the extrapolated line from the original curve. The film diffusion coefficient  $D_f$  (in  $\text{m}^2/\text{s}$ ) can be calculated from the following relation by using the  $k_1$  values;

$$D_f = k_1 \frac{V\delta\bar{C}_\infty}{A} \quad (5)$$

where,  $V$  is solution volume,  $\delta$  is the thickness of liquid film,  $A$  is the specific surface area of the adsorbent and  $\bar{C}_\infty$  is adsorbate concentration in solid phase determined from the intercept of extrapolated line.

The rate constant  $k_2$  (in L/mol s) corresponding to the slow process is determined from the slope of

extrapolated straight lines in Figure 1(b) according to following equation:

$$\ln(1 - F_t) = A - k_2(C_t + \bar{C}_t)t \quad (6)$$

When the particle diffusion contributes on adsorption process by assuming that the diffusion is radial direction following equation can be used to obtain adsorbed fraction;

$$F_t = 1 - \sum_{n=1}^{\infty} \frac{6\alpha(\alpha + 1)}{9 + 9\alpha + \alpha^2 q_n^2} e^{-D_p q_n^2 t / r_0^2} \quad (7)$$

Thus,

$$\ln(1 - F_t) = A - \frac{D_p q_1^2}{r_0^2} t \quad (8)$$

where,  $A = \ln[6\alpha(\alpha + 1)] / (9 + 9\alpha + \alpha^2 q_1^2)$ ,  $r_0$  is mean radius of particles,  $q_n$ 's are the non-zero roots of  $\tan q_n = (3q_n) / (3 + \alpha q_n^2)$  and  $\alpha = (3V) / (4\pi r_0^3)$  represents the volume ratio of external solution to the solid particles. Constant  $k_2$  can be correlated to  $D_p$  with a combination of eqs. 6 and 8 as follows:

$$D_p = k_2 \frac{(C_t + \bar{C}_t)r_0^2}{q_1^2} \quad (9)$$

The calculated values of  $k_1$  and  $k_2$  depending on particle size are presented in Table I. As it is from the Table I,  $k_1$  values  $\sim 10^3$  times higher than  $k_2$  and decrease with increasing particle size. On the other hand,  $k_1$  values increase depending on particle radius. The values of  $D_f$  and  $D_p$  have been calculated according to eqs. (5) and (9) by assuming 18  $\mu$ , 27.5  $\mu$ , and 80  $\mu$  mean particle radii. The magnitude of diffusion coefficients presented in Table I is in consistent with the literatures.<sup>14,15</sup> Using the of  $k_1$  and  $k_2$  values calculated  $q_t$  vs.  $t$  curves according to McKay model are compared to experimental points in Figure 1(a) (dashed lines). Standard deviations

TABLE I  
Kinetic Parameters for U Adsorption on the SPR with Different Particle Sizes

$d \times 10^6$ m	$V/m$ L/g	$k_1 \times 10$ L/mol s	$D_f \times 10^8$ $\text{m}^2/\text{s}$	$k_2 \times 10^4$ L/mol s	$D_p \times 10^{14}$ $\text{m}^2/\text{s}$	$\sigma$	$D_{p(\text{NP})} \times 10^{12}$ $\text{m}^2/\text{s}$	$\sigma$
$d < 40$	0.5	2.41	5.32	2.37	0.01	0.0015	3.24	0.0026
$40 < d < 150$		2.07	3.48	3.61	0.04	0.0007	7.56	0.0010
$d > 150$		0.43	1.20	6.53	1.19	0.0012	25.60	0.0020
$40 < d < 150$	7.5	0.20	0.29	6.25	0.18	0.0174	0.23	0.0367

between calculated and observed  $q_t$  values were calculated from the following relation and presented in Table I.

$$\sigma = \left[ \frac{1}{n_e} \sum_{i=1}^n \left( \frac{q_{t,\text{exp}} - q_{t,\text{cal}}}{q_{t,\text{exp}}} \right)^2 \right]^{1/2} \quad (10)$$

where, the subscripts "exp." and "mod." are the experimental and modeled values of  $q_t$ , respectively, and  $n$  is the number of measurements.

As it is seen in Figure 1(a) and standard deviations in Table I experimental data well predicted by McKay model.

Kinetic parameters obtained for the  $40 \mu < d < 150 \mu$  sizes at a solution/solid ratio of 7.5 L/g are also presented in Table I. The value of  $k_1$  decreases from  $2.07 \times 10^{-1}$  L/mol s to  $2.00 \times 10^{-2}$  L/mol s when  $V/m$  ratio increases from 0.5 to 7.5 L/g whereas  $k_2$  value increases two times. It can be concluded that film diffusion process is lowered at higher  $U$  loadings while particle diffusion increases.

Time dependent elution studies with 0.1 M NaNO<sub>3</sub> solution until 1500 min shows that only 4% of loaded  $U$  is recovered. This may be considered also in experimental errors. Thus, the kinetic models couldn't be applied to the elution data. Similar results have been reported for  $U$  adsorption onto chitosan.<sup>18</sup> Time dependent desorption studies until 48 h in 0.03 M NaNO<sub>3</sub> solution show that very small amount of uranyl ions is removed in the physisorbed water that remained on chitosan after centrifugation. Thus, no chemical desorption was observed.

### Nernst-Plank model

Typical adsorption kinetics is described in terms of fractional attainment of equilibrium  $U_t$  at time  $t$  and determined experimentally as follows:

$$U_t = \frac{q_t}{q_e} \quad (11)$$

To determine  $U_t$  according to Nernst-Plank model the following equation was employed:<sup>16,17</sup>

$$U_t = [1 - \exp(m)]^{1/2} \quad (12)$$

with

$$m = \pi^2 [c_1(\beta P) + c_2(\beta P)^2 + c_3(\beta P)^3], \quad (13)$$

where,  $P = \frac{D_p t}{r_p^2}$ , the constants  $c_1$ ,  $c_2$ , and  $c_3$  are functions of  $\beta$ . The constants were calculated as follows

for  $\beta = 15$  by minimizing standard deviation between experimental and modeled  $q_t$  values.

$$c_1 = -\frac{1}{0.01 + 0.2 \beta^{0.2}} \quad (14)$$

$$c_2 = -\frac{1}{0.1 - 2 \beta^{0.4635}} \quad (15)$$

$$c_3 = -\frac{1}{0.27 + 0.09 \beta^{1.14}} \quad (16)$$

The values of  $D_p$  calculated from Nernst-Plank's approximation are presented in Table I and the calculated curves are compared with experimental points in Figure 1(a). The dependence of  $D_p$  on particle size shows similar trend with McKay model.

A few data are available in the literature related to diffusion coefficients of  $U$ . The reported diffusion coefficients based on one resistance diffusion process (Bt plot) are  $9 \times 10^{-10}$  and  $3.5 \times 10^{-13}$  m<sup>2</sup>/s for clinoptilolite and tin (IV) antimonate, respectively.<sup>19,20</sup> The  $D_p$  values for  $U$  on the SPR calculated from Nernst-Plank model based on similar assumptions are in the range of  $2.3 \times 10^{-13}$  –  $2.56 \times 10^{-11}$  m<sup>2</sup>/s and well comparable with the reported values.

The theoretical curves calculated from both McKay and Nernst-Plank models are in agreement with experimental data points indicating  $U$  adsorption on the SPR is a diffusion-controlled process. The lower standard deviations for McKay model indicate that two-resistance diffusion better describes experimental results rather than single one.

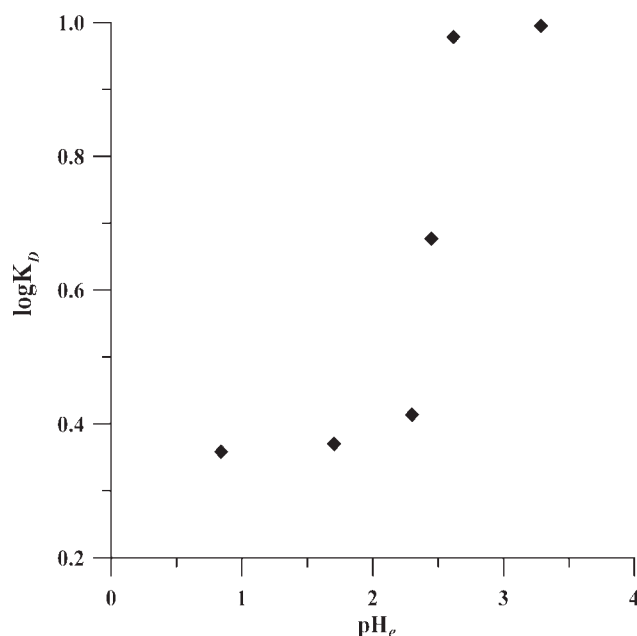


**Figure 2** Equilibrium pH dependency of distribution coefficients at the  $V/m$  ratio of 7.5 L/g.

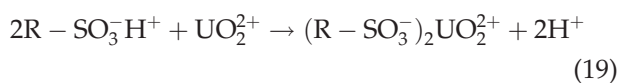
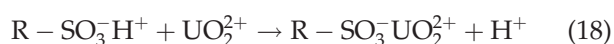
### pH dependency of uranium adsorption

pH dependency of U adsorption has been studied at constant ionic strength of 0.25 mol/L because the changes in ionic strength during pH adjustment strongly affect on  $K_D$  calculated from the following relation.

$$K_D = \frac{F}{1-F} \times \frac{V}{m} \quad (17)$$

The decrease in uranium adsorption after ionic strength adjustment with  $\text{NaNO}_3$  may be attributed to the competition of sodium and uranyl ions for adsorption sites on the SPR.

The dependence of the  $K_D$  values (in L/g) on  $\text{pH}_e$  for U adsorption on the SPR is shown in Figure 2. A sigmoid curve is observed as expected.<sup>21,22</sup> It may be inferred from the following reactions that uranyl adsorption by ion-exchange reactions would be favored by neutralization of  $\text{H}^+$  ions eliminated from sulfonate groups on the resin surface.<sup>23,24</sup>



The numbers of protons released per bound uranyl ion can be calculated from the slope of increasing linear part of  $\log K_D$  vs.  $\text{pH}_e$  curve.<sup>21</sup> The slope of 1.8 indicates coordinative bidentate binding according to eq. (19) rather than monodentate surface complex in eq. (18).

The number of protons released from sulfonate groups increases depending on increasing pH. Uranyl ions are specifically adsorbed on negatively charged sulfonate groups via electrostatic interactions. Amount of U adsorbed increases from 0.087 to 0.21 mol/g when equilibrium pH increases from 0.840 to 3.285. On the other hand, the number of sulfonate groups per unit polymeric chain is 1 wt % (i.e.,  $1.25 \times 10^{-4}$  mol/g).<sup>13,25</sup> This indicates in the presence of solute-solute interactions on adsorbent surface. It is well-known that sodium uranates prepared at different pH medium have polymeric character and the length of polymeric chain depends on pH.<sup>26</sup> This suggests that a uranyl chain forms on bidentate surface complex. The negatively charged sulfonate groups electrostatically interact with U atom of uranyl cation and its O atoms are oriented towards solution phase. Similarly, nonbonding free electron pairs of O atoms are bounded to U atoms of uranyl cation to form a uranyl chain. Thus, two protons are released from the surface per bounded uranyl chain. They might be bound on O atoms on

uranyl chain because pHs of the solutions slightly increase at equilibrium.

### Effect of solution/solid ratio on uranium adsorption and desorption

Effect of solution/solid ratio on the fraction ( $F$ ) of uranium adsorption and desorption is depicted in Figure 3. As it can be seen from the figure the values of adsorbed fraction of U on the SPR slowly decrease from  $\sim 0.90$  to  $\sim 0.85$  in the range of 0.0125 – 5 L/g solution/solid ratio whereas a stronger decrease is observed in 7.5–25 L/g range. However, desorbed fractions of U with water are very low (maximum  $\sim 0.035$ ). This indicates irreversible binding of U on SPR surface.

### Adsorption equilibria

Amount of U adsorbed at equilibrium ( $q_e$ ) has been evaluated from the  $F$  values according to eq. (1) and adsorption isotherm has been constructed in Figure 4(a). As it is seen from the figure an S shaped isotherm is observed. Since initial concentration of U is 0.05 mol/L and the values of  $F$  are nearly constant the part of isotherm corresponding to  $V/m$  range of 0.0125 – 5 L/g  $q_e$  values increases exponentially to form initial concave profile of the isotherm. The slightly convex plateau region of the isotherm corresponds to decreasing  $F$  values in 7.5–25 L/g range. The S shaped isotherm confirms the presence of solute-solute interactions.

Freundlich and Dubinin-Radushkevich isotherm equations can be applied to the equilibrium data of

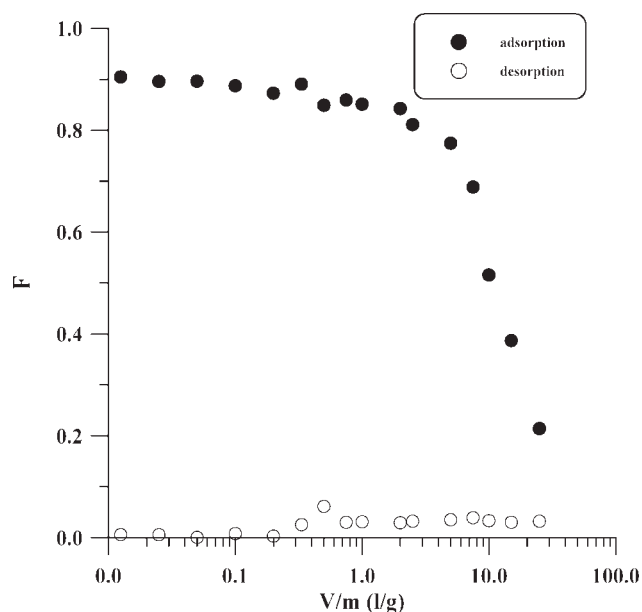


**Figure 3** The change of adsorbed and desorbed fractions of U with solution/adsorbent ratio.

an S shaped isotherm while Langmuir isotherm is applicable only to the L shaped (i.e., Langmuir type) isotherm.

### Freundlich isotherm

The Freundlich adsorption isotherm equation and its linear form can be written as follows:

$$q_e = k_F C_e^n \quad (20)$$

$$\ln q_e = \ln k_F + n \ln C_e \quad (21)$$

where,  $k_F$  and  $n$  are the Freundlich isotherm constants, which are capacity and intensity factors, respectively. Their values have been calculated from the slopes and intercepts of the straight lines of  $\ln q_e$  vs.  $\ln C_e$  plot. As shown in Figure 4(b) linearized Freundlich isotherm gives two straight lines with

decreasing slopes. The Freundlich exponent  $n > 1$  represents the initial part of an S shaped isotherm with concave profile whereas  $n < 1$  value corresponds to convex part of the isotherm. The  $n > 1$  value indicates multilayer adsorption as a result of solute-solute interactions on adsorbent surface while  $n < 1$  corresponds to the slightly increasing plateau region because the Freundlich equation does not into account a finite capacity. However, the value of  $k_F$  for the second region can be used only comparison purposes of adsorption capacities. The value of  $k_F$  of 0.64 mol/g is nearly two times of experimentally attainable capacity of 0.29 mol/g (i.e., 69 g U per g adsorbent). This value is much higher than reported capacities for Safranin T of  $2.9 \times 10^{-4}$  mol/g, for Nile Blue A of  $1.7 \times 10^{-4}$  mol/g and for Brilliant Cresyl Blue of  $1.5 \times 10^{-4}$  mol/g, respectively.<sup>13</sup>

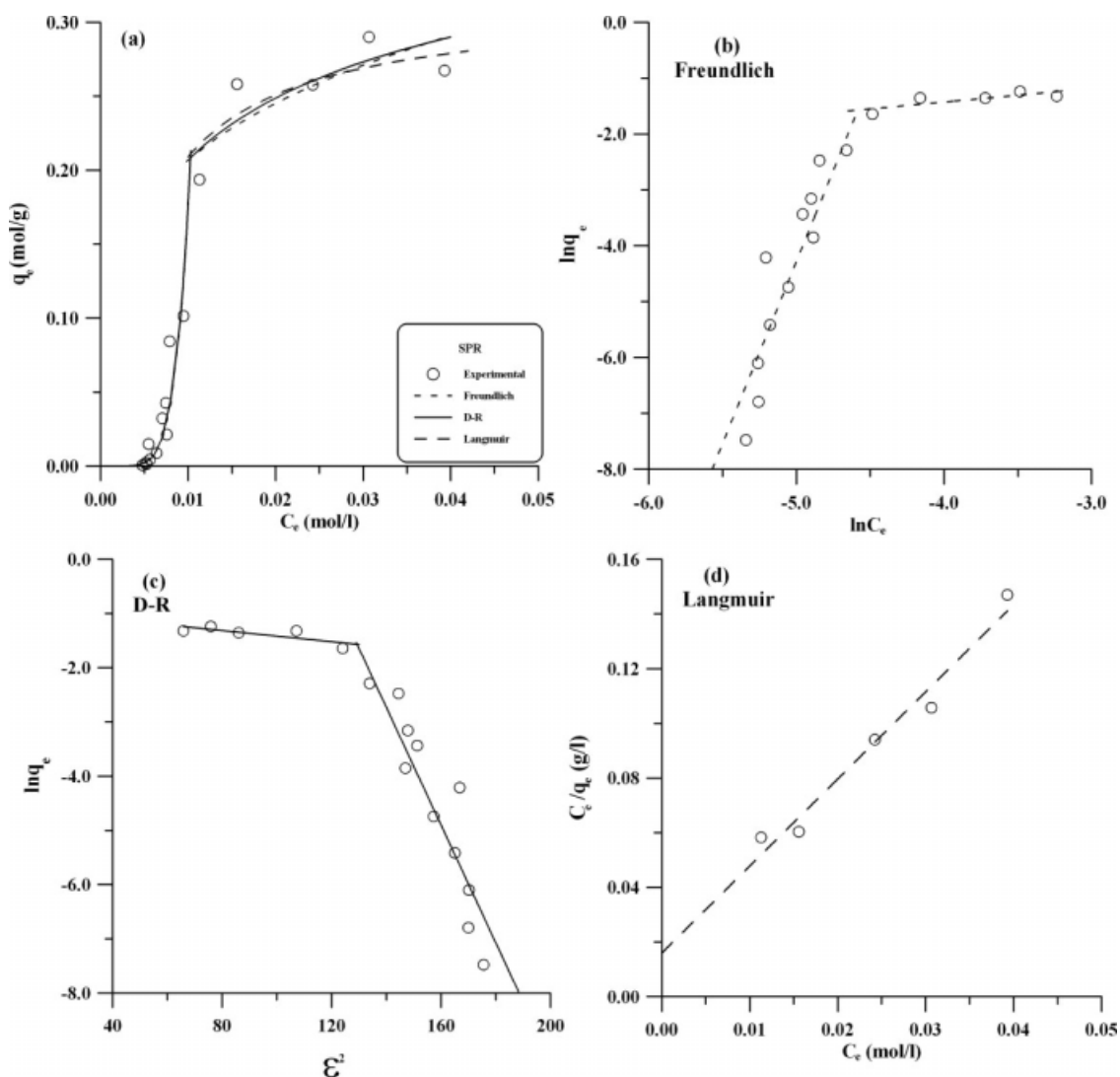


**Figure 4** (a) adsorption isotherm of U adsorption on the SPR, (b) the Freundlich isotherm, (c) the D-R isotherm, (d) the Langmuir isotherm.

TABLE II  
Freundlich, D-R and Langmuir Isotherm Constants for U Adsorption on the SPR

Region	Freundlich			D-R			Langmuir		
	$n$	$k_F$ mol/g	$r$	$E$ kJ/mol	$q_m$ mol/g	$r$	$K_L$ L/mol	$q_m$ mol/g	$r$
1	6.51	$1.98 \times 10^{12}$	0.92	2.1	$2.63 \times 10^5$	0.93	–	–	–
2	0.25	0.64	0.81	9.9	0.41	0.78	$2.02 \times 10^2$	0.31	0.98

### Dubinin-Radushkevich (D-R) isotherm

The D-R isotherm equation can be useful for the calculation of adsorption capacity ( $q_m$ ) when solute–solute interactions on the adsorbent are important. The D-R isotherm equations in following forms have been used,

$$q_e = q_m e^{-K_{D-R}\epsilon^2} \quad (22)$$

$$\ln q_e = \ln q_m - K_{D-R}\epsilon^2 \quad (23)$$

where,  $q_m$  is adsorption capacity of the adsorbent and  $K_{D-R}$  is the constant related to the mean adsorption energy and  $\epsilon$  is the Polanyi potential:

$$\epsilon = RT \ln(1 + 1/C_e), \quad (24)$$

where,  $R$  is the gas constant and  $T$  is the absolute temperature.

The mean adsorption energy ( $E = -\Delta G$ ) is defined as the free energy change when one mole of solute is transferred to the adsorbent surface from infinity in the solution and it can be estimated using constant  $K_{D-R}$  as follows:

$$E = (2K_{D-R})^{-1/2} \quad (25)$$

As it is seen in Figure 4(c), a plot of  $\ln q_e$  vs.  $\epsilon^2$ , allows the estimation of  $q_m$  from the intercept and  $K_{D-R}$  from the slope, respectively. The higher value of  $E$  in Table II shows that U adsorption is more spontaneous in the high loading region. Adsorption energies calculated from the D-R isotherm parameters for U adsorption onto activated charcoal,<sup>27</sup> bentonite composite,<sup>28</sup> molecular sieve,<sup>1</sup> and clinoptilolite<sup>19</sup> have been reported as 4.08, 6.25, 9.11, and 11.18 kJ mol<sup>-1</sup>, respectively. The adsorption energy of 9.9 kJ/mol for the SPR is comparable with the reported data in literature.

Adsorption is sparse at low U loadings, so interactions between uranyl chains are negligible while interactions between adjacent chains may lead a cross-linked network resulting higher free energy change at the plateau region. The proposed interactions between uranyl chains and the sulfonate groups have been presented in Figure 5. Positive charge of the uranyl loaded SPR may be balanced by diffusion of counter ions into the cages. The

strong bonds (dashed bonds in Fig. 5) between U and O atoms cannot be broken for exchanging with Na<sup>+</sup> ions when treated with NaNO<sub>3</sub> solution. Even though the resin cannot be regenerated it can be used as an excellent material for preconcentration before ultimate disposal of U because of its enormous capacity.

Although the predicted adsorption capacity of 0.41 mol/g from the D-R equation is also somewhat higher than that of experimental capacity the theoretical isotherm curves have been successfully calculated by using the isotherm parameters in Table II. A comparison of calculated curves with experimental points indicates that both of the equations are able to adequately predict the equilibrium behavior of U adsorption on the SPR.

### Langmuir isotherm

The Langmuir isotherm equation is another useful model, which allows calculating accurate adsorption

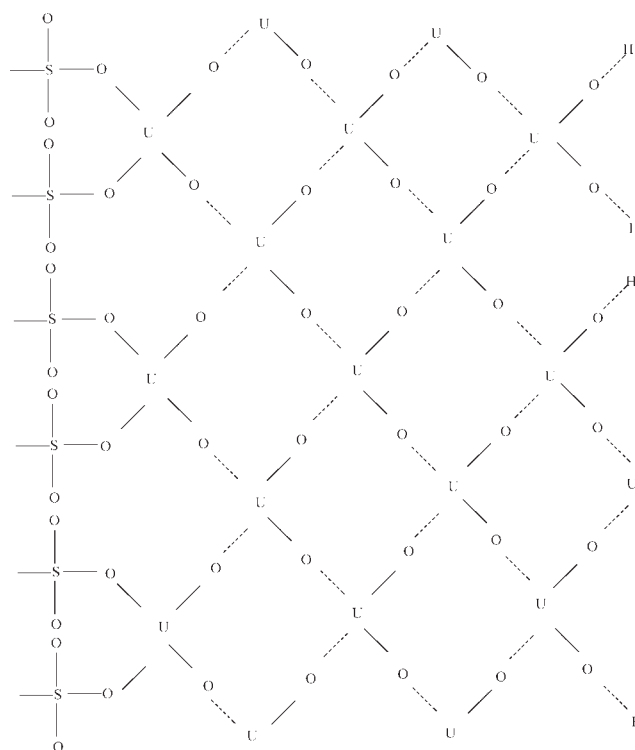


Figure 5 Interactions between uranyl chains and sulfonate groups.

capacity, but it can be applied only to the convex part of the isotherm curve in Figure 4(a).

The Langmuir isotherm equation and its linear form can be represented as follows:

$$q_e = \frac{K_L q_m C_e}{1 + K_L C_e} \quad (26)$$

$$\frac{C_e}{q_e} = \frac{1}{K_L q_m} + \frac{1}{q_m} C_e \quad (27)$$

where,  $K_L$  is the Langmuir adsorption equilibrium constant related to the binding energy. The parameters of  $K_L$  and  $q_m$  for U removal can be calculated from  $C_e/q_e$  versus  $C_e$  plots evaluated from the second part of the isotherm curve. As shown from Figure 4(a), isotherm curve calculated from the Langmuir parameters presented in Table II fits well to the experimental data in plateau region. The Langmuir adsorption capacity of 0.31 mol/g is also well consistent with the experimental adsorption capacity of 0.29 mol/g estimated from the plateau of the isotherm curve.

The reported capacities of some adsorbents for U are as follows: 0.05 g/g for composite bentonite,<sup>28</sup> ~0.23 g/g for Fe and Al modified titanium and zirconium phosphates,<sup>29</sup> 0.23–0.45 g/g for marine algae,<sup>30</sup> 0.30–0.39 g/g for interpenetrating polymer networks (IPNs),<sup>31</sup> 0.307 g/g for cross-linked persimmon peel gel,<sup>32</sup> 0.58 g/g for polyurethane foam loaded with crown ether,<sup>33</sup> 0.76 g/g for benzoylthiourea immobilized on silica gel,<sup>34</sup> 2.38 g/g for hematite,<sup>35</sup> and 29.94 g/g activated charcoal.<sup>27</sup> Adsorption capacity of the SPR of 69 g/g is much higher than those of the reported values.

### Effect of anion of U salt

The amounts of U adsorbed from uranyl-nitrate solution are 0.021 and 0.042 mol/g at the  $V/m$  ratios of 0.5 and 1.0 L/g, respectively. The corresponding values for uranyl acetate solutions are 0.014 and 0.023 mol/g, respectively. U adsorption from uranyl nitrate solution is nearly two times higher than that of uranyl acetate. Since the pH of 0.05 M uranyl acetate solution is ~4 a higher U adsorption is expected. Similar behavior has been reported for Sr adsorption in acetate buffer at the same pH.<sup>22</sup> The great difference of Sr adsorptions between chloride and acetate solutions has been attributed to complex formation with acetate anion.<sup>36</sup> Similarly, coulombic attraction between  $-\text{SO}_3^-$  groups on the SPR surface and  $\text{CH}_3\text{COOUO}_2^+$  should be less than that of  $\text{UO}_2^{2+}$ .

### CONCLUSIONS

Kinetics and equilibrium properties of U adsorption on the SPR have been determined depending on

contact time, solution/adsorbent ratio, particle size and pH.

Kinetic results are well described with both single and two resistance diffusion models. The film diffusion coefficients ( $D_f$ ) calculated from McKay constants based on two-resistance diffusion decrease with increasing particle size whereas particle diffusion coefficients ( $D_p$ ) calculated according to both models increase.

The S shaped isotherm indicates the presence of solute–solute interactions on adsorbent surface. pH dependent experiments reveal that a polymeric uranyl chain forms on the bidentate surface complex.

The equilibrium data are well described with the Freundlich and the D-R isotherm equations. Both equations give two straight lines corresponding to low and high U loadings. The higher free energy change obtained from the D-R parameters indicates that U adsorption is more spontaneous in the second region. This may be arising from interactions between neighboring uranyl chains to form a cross-linked network.

It has been found that the SPR is an excellent material for preconcentration of U before ultimate disposal of radioactive wastes. Since its adsorption capacity of ~0.30 mol/g is extremely high and the loaded U is neither soluble in water nor exchangeable with cations it cannot escape from a breached repository into environment.

The authors thank Tülin Banu İyım, İşil Acar, Saadet Özgümüş from Chemical Engineering Department of Istanbul University for their kind donation of the SPR.

### References

1. Qadeer, R.; Hanif, J.; Khan, M.; Saleem, M. *Radiochimica Acta* 1995, 68, 197.
2. Qadeer, R.; Hanif, J. *Radiochimica Acta* 1994, 65, 259.
3. Vaaramaa, K.; Lehto, J.; Jaakkola, T. *Radiochimica Acta* 2000, 88, 361.
4. Saito, K.; Uezu, K.; Hori, T.; Furusaki, S.; Sugo, T.; Okamoto, J. *AIChE J* 1988, 34, 411.
5. Egawa, H.; Harada, H.; Nonaka, T. *Nippon Kagaku Kaishi* 1980, 1767.
6. Egawa, H.; Harada, H.; Shuto, T. *Nippon Kagaku Kaishi* 1980, 1773.
7. Hirotsu, T.; Katoh, S.; Sugasaki, K.; Takai, N.; Seno, M.; Itagaki, T. *Ind Eng Chem Res* 1987, 26, 1970.
8. Hirotsu, T.; Hori, T.; Furusaki, S.; Sugo, T.; Okamoto, J. *Ind Eng Chem Res* 1987, 26, 1977.
9. Egawa, H.; Nakayama, N.; Nonaka, T.; Sugihara, E. *J Appl Polym Sci* 1987, 33, 1993.
10. Nakayama, N.; Uemura, K.; Nonaka, T.; Egawa, H. *J Appl Polym Sci* 1988, 36, 1617.
11. Egawa, H.; Nonaka, T.; Ikari, M. *J Appl Polym Sci* 2003, 29, 2045.
12. Egawa, H.; Kabay, N.; Shuto, T.; Jyo, A. *J Appl Polym Sci* 1992, 46, 129.



13. İyim, T. B.; Acar, I.; Özgümüş, S. *J Appl Polym Sci* 2008, 109, 2774.
14. Huang, T. C.; Tsai, F. N. *J Inorg Nucl Chem* 1970, 32, 17.
15. Huang, T. C.; Li, K. Y.; Hoo, S. C. *J Inorg Nucl Chem* 1972, 34, 47.
16. Helfferich, F. *Ion Exchange*; McGraw-Hill: New York, 1962.
17. Inglezakis, V. J.; Grigoropoulou, H. P. *J Colloid Interface Sci* 2001, 234, 434.
18. Piron, E.; Domard, A. *Int J Biol Macromol* 1998, 22, 33.
19. Kilincarslan, A.; Akyil, S. J. *Radioanal Nucl Chem* 2005, 264, 541.
20. Badei, M. M. A.; El -Naggar, I. M.; El - Belihi, A. A.; Aly, H. M.; Aly, H. F. *Radiochim Acta* 1992, 56, 89.
21. Anderson, M. A.; Rubin, A. J. *Adsorption of Inorganics at Solid Liquid Interfaces*; Ann Arbor Science: Ann Arbor, 1981.
22. Apak, R.; Atun, G.; Güçlü, K.; Tütem, E.; Keskin, G. *J Nucl Sci Technol* 1995, 32, 1008.
23. Davis, J. A.; Leckie, J. O. *J Colloid Interface Sci* 1978, 67, 90.
24. Davis, J. A.; James, R. O.; Leckie, J. O. *J Colloid Interface Sci* 1978, 63, 480.
25. Yunchao, H.; Fansen, Z.; Hu, Y.; Chunying, L.; Zhaoqiang, W.; Weining, L.; Shukai, Y. *J Appl Polym Sci* 1995, 56, 1523.
26. Maly, J.; Vesely, V. J. *Inorg Nucl Chem* 1958, 7, 119.
27. Qadeer, R.; Hanif, J.; Saleem, M.; Afzal, M. *J Radioanal Nucl Chem Lett* 1992, 165, 243.
28. Donat, R.; Aytas, S. J. *Radioanal Nucl Chem* 2005, 265, 107.
29. Zhuravlev, I.; Zakutevsky, O.; Psareva, T.; Kanibolotsky, V.; Strelko, V.; Taffet, M.; Gallios, G. *J Radioanal Nucl Chem* 2002, 254, 85.
30. Khani, M. H. *Electron J Biotechnol* 2006, 9, 100.
31. Aycik, G. A.; Gurellier, R. *J Radioanal Nucl Chem* 2007, 273, 713.
32. Inoue, K.; Kawakita, H.; Ohto, K.; Oshima, T.; Murakami, H. *J Radioanal Nucl Chem* 2006, 267, 435.
33. Abou-Mesalam, M. M.; El-Naggar, I. M.; Abdel-Hai, M. S.; El-Shahawi, M. S. *J Radioanal Nucl Chem* 2003, 258, 619.
34. Merdivan, M.; Seyhan, S.; Gok, C. *Microchim Acta* 2006, 154, 109.
35. Zeng, H.; Singh, A.; Basak, S.; Ulrich, K. U.; Sahu, M.; Biswas, P.; Catalano, J. G.; Giammar, D. E. *Environ Sci Technol* 2009, 43, 1373.
36. Lurie, J. U. *Handbook of Analytical Chemistry*; Mir Publication: Moscow, 1978.